International Journal of Applied Engineering Research ISSN 0973-4562 Volume 13, Number 7 (2018) pp. 5236-5243

Power Flow Control and Power Quality Improvement in DFIG Based Wind Energy Conversion System Using Neuro Fuzzy System

Maloth Naresh[1*], Umesh Kumar Soni[2] and Ramesh Kumar Tripathi[3]

[1,2,3] Department of Electrical Engineering

[1,2,3] Motilal Nehru National Institute of Technology Allahabad, India

Abstract

Now a days, the renewable energy sources based on wind energy is one of the most accomplished system. The operation and control of the grid side converter of doubly fed induction generator (DFIG) connected to wind turbine to improve the power flow control, stator and rotor control is achieved during unbalance load conditions, the RSC and GSC that are connected back-to-back through a dc-link capacitor. In standalone PV/Wind sources cannot generate power round the clock and all over the year. Due to this reason balance load power is necessary to add battery bank/FC to the generating system. The proposed system is Power Flow Control and Power Quality Improvement in DFIG Based Wind Energy Conversion System Using Neuro Fuzzy System, the phase locked loop (PLL) is synchronized to a reference frequency generated inside the system. The proposed load/battery management system regulates the battery set points for improvement in the performance. The supercapacitor based storage system is used for balance the load at intermittent conditions to satisfy above features. The whole research work and analysis has been carried out in MATLAB/SIMULINK environment for DFIG based on WECS.

Keywords: DFIG, FPGA, FLC, Grid Connected System, Power Control, PLL, Wind Turbine

Nomenclature

DFIG	: Doubly fed induction generator
PWM	: Pulse width modulation
PFC	: Power factor correction
WECS	: Wind energy conversion system
BESS	: Battery Energy Storage System
RSC	: Rotor side converter
GSC	: Grid side converter
PCC	: point of common coupling
IG	: Induction Generator
FPGA	: Field Programmable Gate Array
PLL	: Phase Locked Loop

I. INTRODUCTION

In recent years, the Renewable Energy based energy based on wind energy system, conventional electric power system to fulfill the gap between electrical power generations and its demand, is leading to continuous enhancement of short circuit current [3, 4]. In Hybrid Renewable Energy Sources (HRES) fuel are plentiful, freely and unlimited hence distribution power generated by the hybrid systems. The many researcher efforts have been devoted to improve the performance of DFIG system under disturbed system [5, 6]. The main benefit of the generator is to supply power both at lagging and leading power factors. The other benefit is the control of the rotor voltages and currents enable the IM to remain synchronized with the grid at the same time as the wind turbine speed varies. An enhanced sensorless control for doubly fed induction generator [7], the PLL model basically used for synchronization of closed loop RF control signals, recover a signal from a noisy communication channel & generate a stable frequency at digital logic circuits [8, 9].The frequency range more tracking can be performed by a Phase locked loop is frequently somewhat limited the phase variation an fault signal of the magnitude to make a PLL oscillator to its changeable frequency ranges can be higher[11-14].

The main drawbacks associated with the vertical axis turbines are lower efficiency and higher torque fluctuations compared to the horizontal axis turbines. Currently, only horizontal axis marine current turbines have been used in most of the large-scale tidal plants capacity over 500 kW. The working principles of marine current turbines and wind turbines are similar because both are driven by the flowing mass of the wind and marine current in geographical locations where strong wind and marine currents are available. Currently, in many countries, the marine current turbine technology has been successfully installed in the coastal areas and they are further developing to tap more power mainly in European countries [15]. Recently, both ocean and wind energies have been integrated together in the United Kingdom [16-18]. The main sustainable power sources are PV/Wind power likely discontinuous properties of PV/Wind sources, in standalone system need power backup devices in a HPS. In this study, HPS combination of different renewable sources likes PV, fuel cell, and batteries. In general power flow control is used for managing the power sharing between the various energy sources.

The dc-dc step-up converter is high efficiency at low voltage of PV/FC hybrid system, through switching actions. The main control methods are voltage mode and current mode. The dc-dc step-up converter is operating CCM and DCM. Most frequently a Pulse Width Modulation (PWM) method is considered suitable among various switching control methods. In presented study, the feasibility and effectiveness of the presented method is confirmed by the measured data from a large wind farm. The authors in [24] demonstrate use of 10 MW and 20 kHz used for PV/Wind/FC modular structure of the inverter. The power distribution between RES and load through a storage backup system to balance the load using adaptive neuro-fuzzy inference system (ANFIS) in PV/Wind/FC/battery system is discussed in this chapter. The dynamic model consists of PV, Wind, FC, storage system, converters and controllers for ensuring the continuous power supply for load demand. The DFIG are operated in generating mode if its speed is going past the PLL at voltage conditions for synchronous speed i.e. at super-synchronous speed. As per the characteristics of wind turbine, wind speed of 10 m/s corresponds to 0.75 pu turbine output power. Here base kVA is 275 kVA so actual turbine output power is 206.25kW (.75*275=206.25). However, 200kW power is available on the output side of wind energy conversion system due to losses in induction generator. Since the main load requires only 50 kW so 150 kW must be absorbed by the secondary load in order to maintain a constant frequency operation. In this study, the performance of FPGA in enhancing operation and control of DFIG based wind energy system.

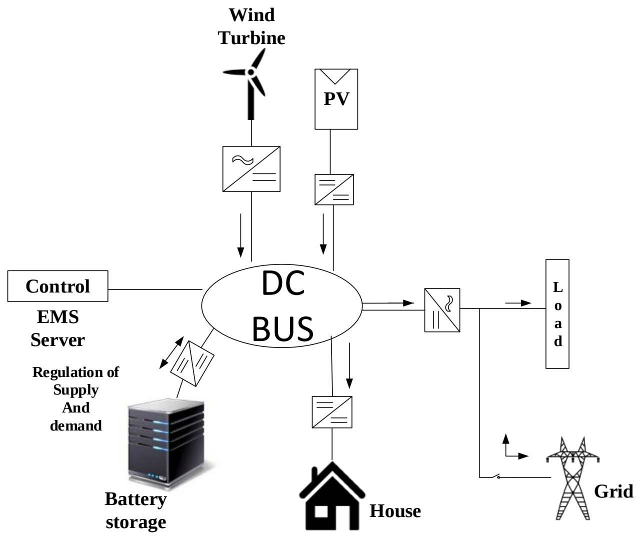

Figure 1. Basic Diagram of DC Microgrid Architecture.

The incorporation of a Wind, PV system BESS with an FC is a viable option for continuous uninterruptable power supply. Thus, the PV-FC with the integration of a BESS is integrated as an HPS is connected to the DC bus system as exposed Fig.1. Further, at the PCC for the issue of PQ in the distribution system is a concern. The systems comprised of PV/Wind and FCs is mostly based on grid-connected converters as interface to the grid. PQ mitigation [25] exploits the capabilities of the dc-ac converter in a renewable power generation system.

WIND ENERGY SYSTEM

A. Wind energy Fundamentals

The fixed speed and variable speed operation is possible. In fixed speed operation of WT, there is direct interconnection between wind generator and grid. Power electronic converters are used to control the generator for variable speed operation. Kinetic energy associated with a moving mass (air in this case) is given by [15]

$$E = \frac{1}{2} m v^2 \quad (1)$$

Where, E is energy contained in air, m is mass of air and v is velocity of air. Now, the wind power of can be calculated by derivation of wind energy (assuming wind velocity to be constant).

$$\frac{dE}{dt} = P_a = \frac{1}{2} v^2 \frac{dm}{dt} \quad (2)$$

$$dV = A.dl \quad (3)$$

$$v = \frac{dl}{dt} \quad (4)$$

$$\frac{dm}{dt} = \frac{d(\rho V)}{dt} = \rho \frac{dV}{dt} = \rho A \frac{dl}{dt} = \rho A v \quad (5)$$

Now power contained in air is given by following equation

$$P_a = \frac{1}{2} \rho A v^3 \quad (6)$$

Where P_a: the power carried in wind in watts, ρ: density of air (assumed to be constant), A: swept area in (meter^2), V: volume of air and v: velocity of air (or wind) without any interference in rotor. The Power coefficient is given

$$C_p = \frac{P_{wind\ turbine}}{P_a} \quad (7)$$

$$P_{wind\ turbine} = \frac{1}{2} \rho C_p A V^3 \quad (8)$$

The maximum value of C_p is 16/27 i.e. 0593 as per Betz limit, and hence no wind turbine. The tip speed ratio is defined as below,

$$\lambda = \frac{v_{rotor}}{v_{wind}} = \frac{r_b w}{v_{wind}} \quad (9)$$

B. Fixed speed wind turbine systems

These wind turbines are directly connected to utility grid without any power electronic converter. The active power control is limited aerodynamically by stall or pitch control. This configuration requires an induction generator with direct grid connection is known as the ‘Danish concept’.

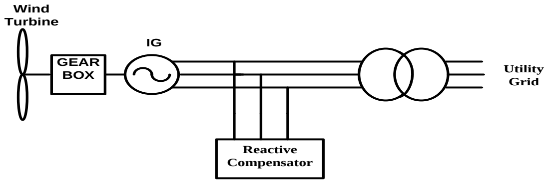

(a)

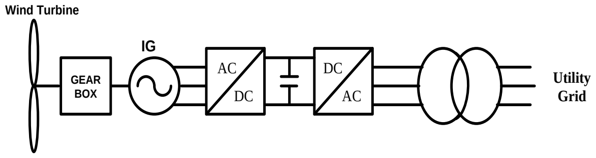

(b)

Figure 2: (a) Fixed speed wind power system, (b) Variable speed wind power system IG.

C. *Variable speed wind turbine system*

These wind turbines are connected to utility grid with help of power electronic converters and hence in this system the generator operates absolutely independently because the DC-link uncouples the generator from grid. However, the generated power must pass the power converter and as a result there are higher losses compared to DFIG (doubly fed induction generator). But a higher performance can be achieved. So reactive and active power is controlled and reactive power can be provided even if there is no wind.

RENEWABLE ENERGY SOURCES

The 2MW wind turbine is made with two blades three phases DFIG, the WES provides a voltage higher than the DC bus voltage those value is variable speed and depend on the wind speed. The DFIG contains of IG, the stator of which connected directly to the grid and is connected to a back to back converter of DFIG in compares the variable speed generator. The supercapacitor storage system used for balance the load at intermittent conditions is considered for the modeling of DFIG shown in Figure. 3, and the control strategy of bidirectional DC/DC converter is shown in Figure 4 The system modeled by a 2 MW DFIG based wind energy system using FPGA, are connected to the common collector platform (PCC).

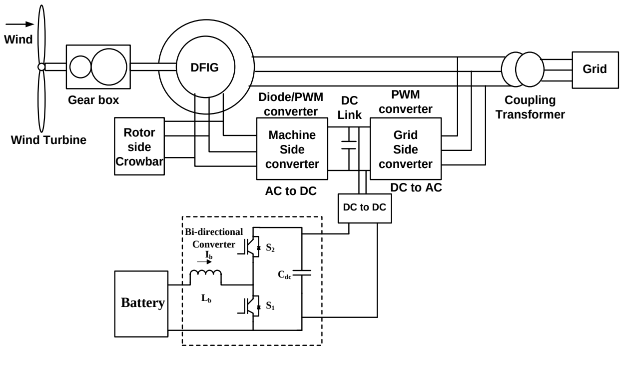

Figure 3. Proposed Diagram of isolated WECS.

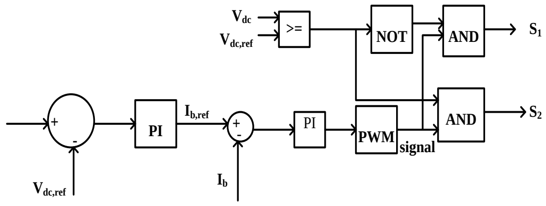

Figure 4. Control strategy of bidirectional DC/DC converter

A. *DFIG Modelling and Control*

General the doubly fed induction generator based wind energy system is shown in Fig 1. The DFIG is considered as one of the important technique useful in wind power systems, its main benefit is to adjust the speed of large system with power converters The RSC is considered and the DC-link is maintained at constant voltage. The equivalent circuit of a DFIG can be expressed in the rotating reference frame, as exposed in Fig. 2. The electric machine model refereed to a rotating reference frame (stator flux or stator voltage) can be summarized using the following set of equations.

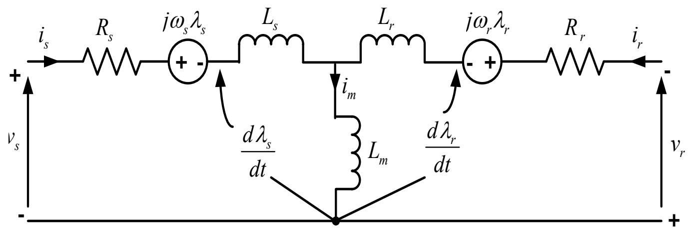

Figure 5. Space vector equivalent circuit of a DFIG in the rotating reference frame.

$$v_s = \frac{d\lambda_s}{dt} + R_s i_s + j\omega_s \lambda_s \tag{10}$$

$$v_r = \frac{d\lambda_r}{dt} + R_r i_r + j\omega_r \lambda_r \tag{11}$$

$$\lambda_s = L_s i_s + L_m i_r \tag{12}$$

$$\lambda_r = L_r i_r + L_m i_s \tag{13}$$

where v_s, i_s, v_r, and i_r are the stator and rotor voltage and current vectors, R,L represent resistance and inductance and the subscripts "s""r" are stator and rotor respectively, Lm is the magnetization inductance, ω_s is the synchronous angular speed, ω_r is the electrical angular speed of the rotor current and λ_s and λ_r are the stator and rotor fluxes. Therefore the rotor electrical angular speed can be calculated using:

$$\omega_r = \omega_s - \omega_{mec} \tag{14}$$

where ω_{mec} is the mechanical speed.

The electromagnetic torque formed by DFIG is

$$T_e = \frac{3}{2} P_p \, \mathrm{R_e}(\lambda_s . i_s) = \frac{3}{2} P_p (\lambda_{sd} . i_{sq} - \lambda_{sq} . i_{sd}) \qquad (15)$$

The active and reactive power of rotor & stator of the DFIG

$$\left. \begin{array}{l} P_s = V_{ds} . i_{ds} + V_{qs} . i_{qs} \\ Qs = V_{qs} . i_{ds} + V_{ds} . i_{qs} \end{array} \right\} \qquad (16)$$

The wind turbine is modeled from the following system equations [9, 10],

$$T_w = \frac{1}{2} . \rho . S . n^3 \qquad (17)$$

$$T_w = \frac{1}{2} . \rho . S . C_p(\lambda, b) . n^3 \qquad (18)$$

$$\lambda = \frac{\Omega_t . R}{n} \qquad (19)$$

$$C_p(\lambda, b) = a_1 \left(\frac{a_2}{\lambda_1} - a_3 b - a_4 \right) e^{-a_5/\lambda_1} + a_6 \lambda \qquad (20$$

Where ρ is the air density, n is the rotor disk radius, C_p is power coefficient, pitch speed ratio (λ) and pitch angle (b).

In case of wind-speed under the rated value for a turbine, the control objective of most DFIG-based turbines is to maintain the power coefficient of the turbine at the optimal value that can be achieved indirectly by controlling the electromagnetic torque of the electric machine [12].

The space vectors in different reference frames. The α-β axes representing the stationary reference frame are orthogonal to each other with the stationary α-axis being in phase with the stator a-axis.

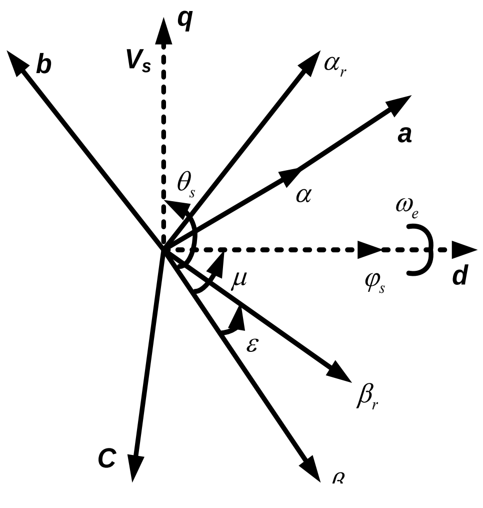

Figure 6. Space vector diagram.

B. Rotor Side converter (RSC)

The RSC is regulated the real and reactive power of the stator. The q-axis control the current loop of real power and d-axis is regulates the flux by controlling the reactive power flow. The control diagram of RSC is shown in Figure.7.

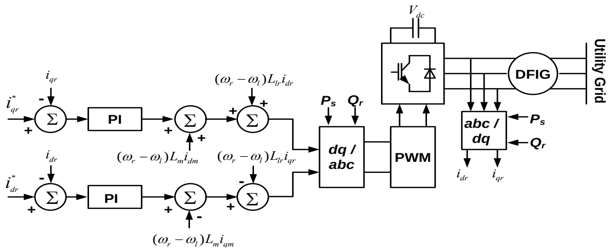

Figure 7. Control Diagram of RSC

The reference for rotor current is written as,

$$i_{qr}^* = -\frac{2}{3} \left[\frac{P_s^*}{v_{qs}} \right] + i_{qfe} + i_{qm} \qquad (21)$$

$$i_{dr}^* = -\frac{2}{3} \left[\frac{Q_s^*}{v_{qs}} \right] + i_{dfe} + i_{dm} \qquad (22)$$

C. Grid Side Converter (GSC)

A general control block diagram of GSC is regulating the DC link voltage and reactive power flow exchanged through the grid. The voltage controller is given output current situation for d-q axis real power balance of the ac & dc side of the power circuit. The control diagram of grid side converter is shown in Figure.8.

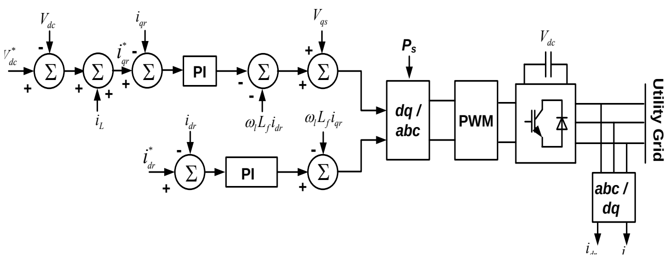

Figure 8. Control Diagram of GSC

D. Control of the BESS

The configuration of BESS as shown is Figure. 9. Here the dc-dc converter, and used two IGBT switches S1 and S2. This configuration is working two different modes, boost and buck converter. When witch S1 is on the dc-dc converter operate buck converter and when switch S2 is on dc to dc converter operate boost converter. The duty ratio of the buck mode is written as [24].

$$D_1 = \frac{V_{sc}}{V_{dc}} \qquad (23)$$

$$D_2 = 1 - D_1 \tag{24}$$

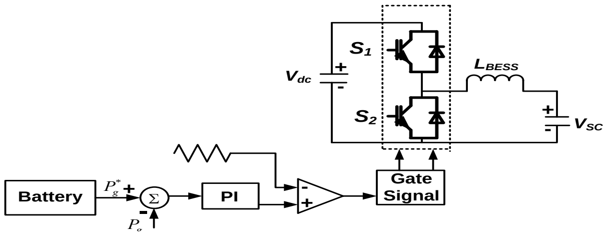

Figure 9. Control block Diagram of BESS

E. Phase Lock Loop (PLL)

The PLL is a linear feedback control system it can be generate an output signal which as the same frequency and phase as the input reference signal. PLL model basically used for synchronization of closed loop RF control signals, recover a signal from a noisy communication channel & generate a stable frequency at digital logic circuits.

ARCHITECTURES OF ANFIS

ANFIS architectures show both the Sugeno and Tsukamoto fuzzy models. Data driven methods for the synthesis of ANFIS are commonly based on cluster a training set models of the unknown function to be approximated. In cases where the numerical model is not accessible the system inquiry becomes extremely troublesome. The prime inherent advantage related with the soft computing procedures of not requiring a numerical model has been a motivating factor for thought in proposed work. Proposed ANFIS controller for power management system (PMS) is more superior in the improvement of dynamic stability of the system than the compared PI, controller. The proposed load/battery management system regulates the battery set points for improvement in the performance.

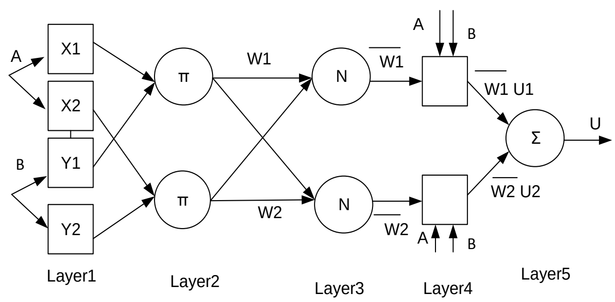

Figure 10. Architectures of ANFIS

SIMULATION AND RESULTS

The performances of the study Standalone operation of wind turbine The proposed system is DFIG based on wind energy system using FPGA, is synchronized to phase locked loop (PLL) to a reference frequency generated inside the system as shown in Fig.1. The simulation was carried out in MATLAB/Simulink and FPGA. The simulation parameters are exposed in Table I.

Table 1. Simulation Parameters

Parameters	Values
Induction generator	275kVA, 480V
Rated capacity	2 MW
Rotor speed (variable)	8.5−15.3 r/min
Nominal stator voltage	4.16 kV,
Capacitor	20mF
LBESS	50mH
supercapacitor bank	2 kV
Rated Frequency	50 Hz
FPGA Simulation Time	25e-7

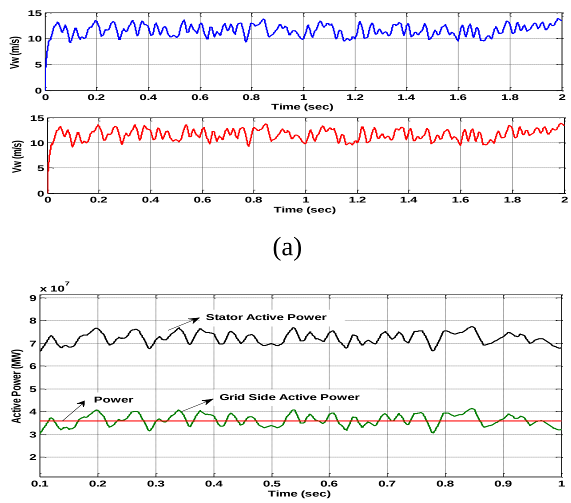

(a)

(b)

Figure 11: (a) Wind Speed at different stage, **(b)** Active Power of wind form.

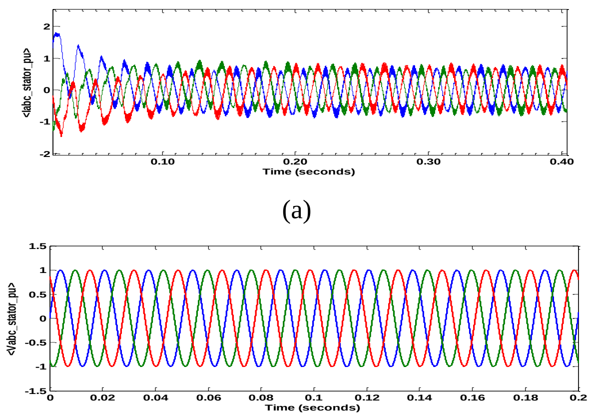

(a)

(b)

Figure 12: (a) Stator Current, **(b)** Stator Voltage

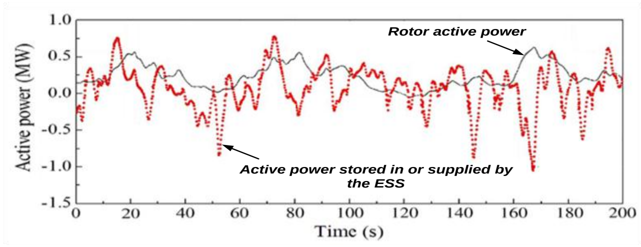

(a)

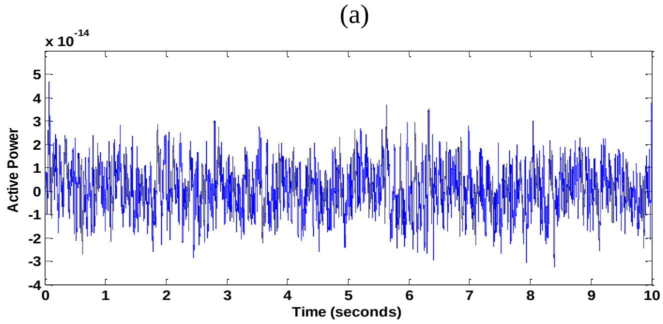

(b)

Figure 13: (a) Rotor active power and active power stored in or supplied by the BESS, **(b)** Active Power of wind turbine

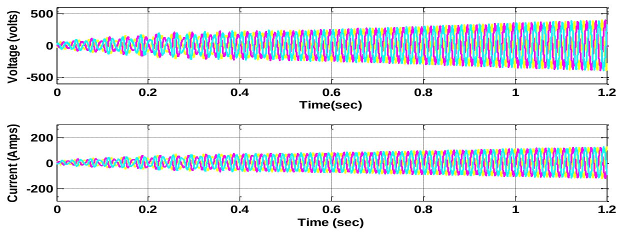

(a)

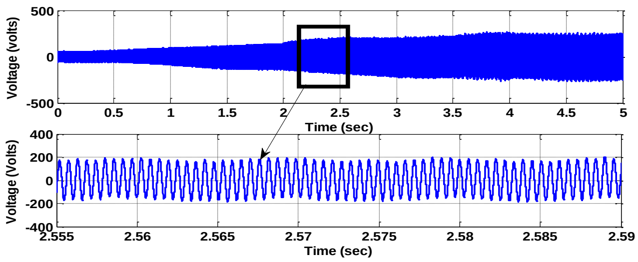

(b)

Figure14 (a) Voltage and Current waveform at load terminal of wind power system. **(b)** Voltage at measured at PCC

DESCRIPTION OF SYSTEM PRESENTED AND ITS SIMULATION

The power flow and the speed variation of wind turbine waveform at different stages as shown in Figure 11(a) and the total stator real power, grid side real power measured at PCC Figure 11(b) and when the some disturbance of the wind that time sum fluctuation of total wind output reactive power at PCC exposed in Figure. 13. The stator current & voltage waveform shown in Figure. 12(a) and Figure 12(b). The RSC active Power and GSC active power for stored or supplied the BESS shown in Figure. 13(a). In Figure 14(a) voltage and current observed the after 0.8 sec voltage and current is normal state. In Figure 14(b) is shown the voltage at measured at PCC. Here also same position of voltage is after 2.5 sec voltage is normal state. Figure 13(b) is shown the active power of wind turbine. Here, induction machine operates in generating mode with super-synchronous speed of 1.011 pu. As per the characteristics of wind turbine, wind speed of 10 m/s corresponds to 0.75 pu turbine output power. Actual turbine output power can be obtained multiplying the per unit value to its base value. Here base kVA is 275 kVA so actual turbine output power is 206.25kW (.75*275=206.25). However, 200kW power is available on the output side of wind energy conversion system due to losses in induction generator. Since the main load requires only 50 kW so 150 kW must be absorbed by the secondary load in order to maintain a constant frequency (50 Hz) operation. The output power PV, FC, Battery and load demand as shown in figure 15, the battery state of charge up to 40% charge battery as shown in figure 16, and battery voltage and battery current is produced the battery as shown in figure 17, Waveform of main load connected to wind power system as shown in figure 18 and finally output power produced by wind turbine is as shown in figure 19.

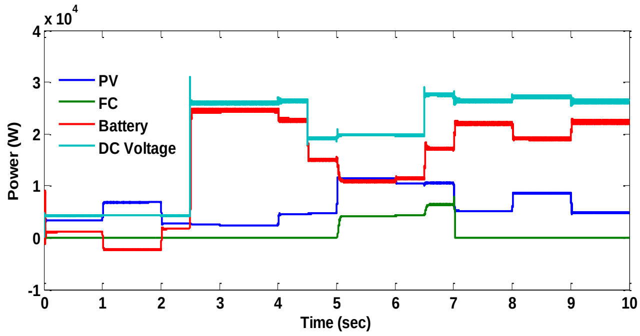

Figure 15: Output power PV, FC, Battery and load demand.

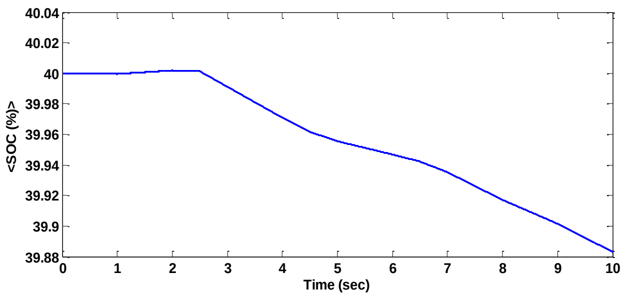

Figure 16: Battery SOC.

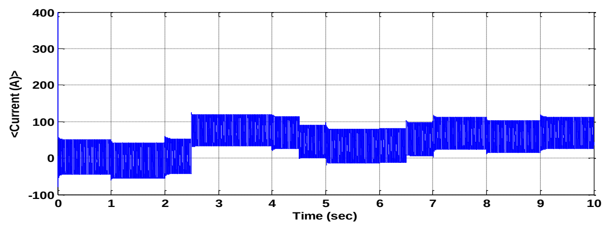

(a)

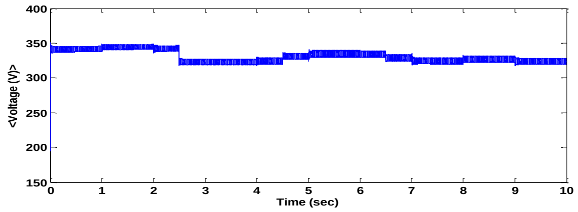

(b)

Figure 17: Battery voltage and Battery current

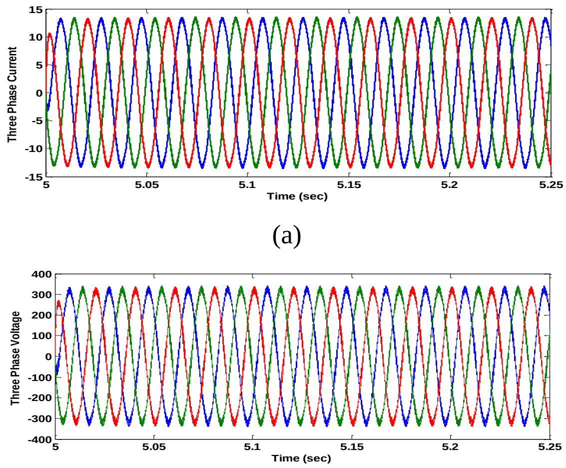

(a)

(b)

Figure 18: Waveform of main load connected to wind power system.

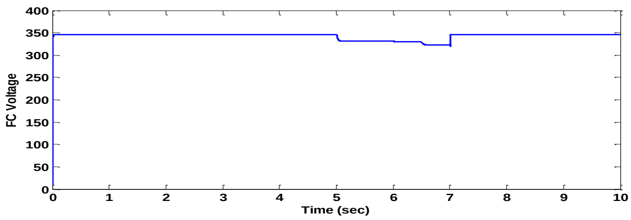

Figure 19: Output power produced by wind turbine

CONCLUSION

The operation and control of the grid side converter of DFIG connected to WT to improve the power flow control, stator and rotor control is achieved during unbalance load conditions, the power flow control and power quality improvement in DFIG based wind energy conversion system using neuro fuzzy system, the phase locked loop (PLL) is synchronized to a reference frequency generated inside the system. The proposed load/battery management system regulates the battery set points for improvement in the performance. Simulation studies have been wind farm with DFIG wind turbines to verify of the proposed scheme, the RSC and GSC that are connected back-to-back through a dc-link capacitor. The power sharing strategy among components consists in the HPS with FLC has been developed. The battery storage system is successful controlled by a bidirectional converter and maintained SOC level within limits.

REFERENCES

[1] S. Bull. 2001. Renewable Energy today and tomorrow. Proc. IEEE, vol. 89, no. 8, pp. 1216-1226.

[2] I.dincer. 2000. Renewable Energy and suitable development: A crucial review *Renew sustain energy rev*, vol.4, no.2 pp. 157-175.

[3] *U.S. Department of Energy,* 20% Wind Energy By 2030: Increasing Wind Energy's Contribution to U.S. Electricity Supply., Jul. 2008.

[4] D. D. Marquezini, D. B. Ramos, R. Q. Machado, and F. A. Farret. 2008. Interaction between proton exchange membrane fuel cells and power converters for AC integration. *IET Renewable Power Gener.,* vol. 2, no. 3, pp. 151–161.

[5] A. Barin, L. F. Pozzatti, L. N. Canha, R. Q. Machado, A. R. Abaide, and G. Arend. 2010. Electrical power and energy systems multi-objective analysis of impacts of distributed generation placement on the operational characteristics of networks for distribution system planning. *Int. J. Elect. Power Energy Syst.,* vol. 32, no. 10, pp. 1157–1164.

[6] W. Qiao and R. G. Harley. 2008. Grid connection requirements and solutions for DFIG wind turbines. *In Proc. IEEE Energy Conf., Atlanta*, GA, Nov. 17–18, pp. 1–8.

[7] [7]. R. Piwko, D. Osborn, R. Gramlich, G. Jordan, D. Hawkins, and K. Porter. 2005. Wind energy delivery issues: Transmission planning and competitive electricity market operation. *IEEE Power Energy Mag*., vol. 3, no. 6, pp. 47–56.

[8] F. Blaabjerg, R. Teodorescu, M. Liserre, and A. V. Timbus. 2006. Overview of control and grid synchronization for distributed power generation systems. *IEEE Trans. Ind. Electron*., vol. 53, no. 4, pp. 1398–1409.

[9] L. Landberg, G. Giebel, H. A. Nielsen, T. Nielsen, and H. Madsen. 2003. Shortterm prediction—An overview. *Wind Energy,* vol. 6, no. 3, pp. 273–280.

[10] P. Rodriguez, A. V. Timbus, R. Teodorescu, M. Liserre, and F. Blaabjerg. 2007. Flexible active power control of distributed power generation systems during grid faults. *IEEE Trans. Ind. Electron.,* vol. 54, no. 5, pp. 2583– 2592

[11] T. Hornik and Z. Qing-Chang. 2011. A current-control strategy for voltage source inverters in microgrids based on H∞ and repetitive control. *IEEE Trans. Power Electron*, vol. 26, no. 3, pp. 943–952.

[12] J. P. Barton and D. G. Infield. 2004. Energy storage and its use with intermittent renewable energy. *IEEE Trans. Energy Convers*, vol. 19, no. 2, pp. 441– 448.

[13] D. Rastler. 2009. Electric energy storage, an essential

asset to the electric enterprise: Barriers and RD&D needs. California Energy Commission Staff Workshop Energy Storage Technol, Policies Needed Support California's RPS Goals 2020, Sacramento.

[14] H. Kim, T. Yu, and S. Choi. 2008. Indirect current control algorithm for utility interactive inverters in distributed generation systems. *IEEE Trans. Power Electron,* vol. 23, no. 3, pp. 1342–1347.

[15] C. Abbey and G. Joos. 2007. Supercapacitor energy storage for wind energy applications. *IEEE Trans. Ind. Appl*, vol. 43, no. 3, pp. 769–776.

[16] JB. S. Borowy and Z. M. Salameh. 1997. Dynamic response of a stand-alone wind energy conversion system with battery energy storage to wind gust. *IEEE Trans. Energy Convers*, vol. 12, no. 1, pp. 73–78.

[17] M.-S. Lu, C.-L. Chang, W.-J. Lee, and L. Wang. 2009. Combining the wind power generation system with energy storage equipments. *IEEE Trans. Ind. Appl,* vol. 45, no. 6, pp. 2109–2115.

[18] A. Yazdani. 2007. Islanded operation of a doubly-fed induction generator (DFIG) wind-power system with integrated energy storage. *In Proc. IEEE Canada Elect. Power Conf., Montreal, QC, Canada,* Oct. 25–26, pp. 153–159.

[19] Maloth Naresh, Navneet Kumar Singh and Asheesh Kumar Singh. 2016. Superconducting Fault Current Limiter for Grid Connected Power System Protection. 2016 IEEE International Conference on Industrial Technology (ICIT), pp. 576-581.

[20] Venkata rama raju rudraraju, nagamani Chilakapati and G Sravana Ilango. 2015. A stator Voltage Switching Strategy for Efficient low speed operation of DFIG Using Fractional Rated converters. *Journal of Renewable Energy*, vol. 81, pp. 389–399.

[21] Singh Badre Bossoufi, mMohammed Karim, Ahmed Lagrioui, Mohammed Taoussi and Aziz Derouich. 2015. Observer backstepping control of DFIG-Generators for wind turbine variable speed: FPGA based implementation. *Renewable Energy,* vol.81, no .1, pp.903-917.

[22] Najafi Hamid Reza and Dastyar Farshad. 2013. Dynamic maximum available power of fixed speed wind turbine at islanding operation. *Electrical power and energy system*, vol. 47, pp. 147–156.

[23] Liyan Qu and Wei Qiao. 2011. Constant Power Control of DFIG Wind Turbines with Supercapacitor Energy Storage. *IEEE Transactions on Industry Applications*, Vol. 47, No. 1, pp. 359–367.

[24] I.dincer. 2000. Renewable Energy and sustaible development: A crucial review. *Renew sustain energy rev,* vol.4, no.2 pp. 157-175.

[25] A. Kuperman, U. Levy, J. Goren, A. Zafranski and A. Savernin. 2011. High Power Li-Ion Battery Charger for Electric Vehicle. *In: Proc. 7th Int. Conf. Workshop Compatibility and Power Electron.(CPE 2011),* Jun.1-3, pp. 342-347.

[26] J. Morren and Sjoerd W. H. de Haan. 2007. Short-Circuit Current of Wind Turbines with Doubly Fed Induction Generator. *IEEE Trans. on Energy Conversion*, vol. 22, no. 1.